Mass cytometry-based identification of a unique T-cell signature predicting childhood AA

Short title: T-cell signature in paediatric AA

Hartmann Raifer[1,2]*, Axel R. Schulz[3]*, Johanna Theodorou[4,5]*, Addi Romero[1], Andreas Böck[4], Wilhelm Bertrams[5,6], Bernd T. Schmeck[5,6], Michael Lohoff[1], Hyun-Dong Chang[3,7], Bianca Schaub[4,5 #], Henrik E. Mei[3#], Magdalena Huber[1#]

[1]Institute for Medical Microbiology and Hospital Hygiene, University of Marburg, 35043 Marburg, Germany

[2]Core Facility Flow Cytometry, University of Marburg, 35043 Marburg, Germany

[3]German Rheumatism Research Center (DRFZ), an Institute of the Leibniz Association, 10117 Berlin, Germany

[4]Pediatric Allergology, Department of Pediatrics, Dr von Hauner Children's Hospital, University Hospital, LMU Munich, 80337 Munich, Germany

[5]Member of the German Center of Lung Research, (DZL), Germany

[6]Institute for Lung Research and Department of Pulmonary and Critical Care Medicine, Universities of Giessen and Marburg Lung Center, Philipps-University Marburg, Member of the German Center for Lung Research (DZL) and the German Center for Infection Research (DZIF), 35043 Marburg, Germany

[7]Technische Universität Berlin, Institute of Biotechnology, Chair of Cytometry, 13355 Berlin, Germany

*****These authors contributed equally to this work

#These authors jointly directed this work

Acknowledgments

This work was generously supported by the Else Kröner-Fresenius-Stiftung (Research group: “Functional, therapy-aimed clustering of T-cell sub-phenotypes across plasticity”). MH is also supported by the Deutsche Forschungsgemeinschaft (DFG) (HU-1824/9-1, HU-1824/7-1, HU-1824/5-1). BS is supported by grants from BMBF 01GL1742A, DFG (DFG-SCHA 997/3-1, DFG-SCHA 997/7-1, DFG-SCHA 997/8-1), from SFB TR22, grants Comprehensive Pneumology Center. JT is supported by grants from the DFG (DFG-SCHA 997/7-1). AB is supported by grants from BMBF (01GL1742A).

Abstract

Background: Allergic asthma (AA) in childhood is characterized by a dominance of type 2 immunity and inefficient counter-regulation by type 1 immunity and/or Tregs among other mechanisms. However, a detailed analysis of T cells associated with paediatric AA is still needed.

Methods: High-dimensional mass cytometry, algorithmic analysis and manual gating were applied to define the peripheral T-cell signature in treatment-naïve childhood AA.

Results: The analysis revealed a changed T-cell profile in children with AA in comparison to healthy controls (HC) consisting of: (i) a lower frequency of memory $CD8^+$ T cells, (ii) an overrepresentation of $TIGIT^+ICOS^+$ Th2 cells connected to a more symptomatic disease with allergic comorbidity and eosinophilia, and (iii) an altered Treg compartment. Within Tregs, the naïve/resting fraction was enriched in children with AA vs HC, it associated inversely with memory $CD8^+$ T cells, and was linked to a lung function decline. Moreover, the ratio of $TIGIT^+ICOS^+$ Th2 cells to dysbalanced effector (e)Treg clusters significantly associated with eosinophilia. Thus, dysregulated Treg fractions were linked to a lung function and, on the other hand, to eosinophilia via $TIGIT^+ICOS^+$Th2 cells. The association of altered Treg clusters with the AA phenotype in ROC analysis underscored the importance of changes in the Treg compartment.

Conclusions: Our approach identifies a unique T-cell signature of childhood AA and provides insights for pathophysiological involvement of dysbalanced Tregs, $TIGIT^+ICOS^+$ Th2 cells and $CD8^+$ T memory cells. This can be useful for immunomonitoring, immunomodulation and for further studies in childhood AA.

Key words:

allergic asthma,

childhood,

clinical disease parameters,

CyTOF,

T-cell subpopulations.

Word count: 3.443

Introduction

Asthma is a chronic inflammatory disease leading to airway hyperresponsiveness, shortness of breath, wheezing and cough. This complex disorder affects more than 300 million people worldwide and can be classified into several endotypes based on the inflammatory cell profile and presence or absence of allergy.[1,2] Approximately 40% of patients with severe asthma develop a type 2 pattern of inflammation with activation of mast cells, mucus hyperproduction, infiltration and activation of eosinophils as well as increased production of IgE by B cells.[3,4] This type of asthma is driven by $CD4^+$ T helper 2 (Th2) cells expressing the transcription factor (TF) GATA3 and producing IL-4, IL-5 and IL-13.[1] Type 2 mediated allergic asthma (AA) starts frequently during early childhood occurring in more than 80% of asthmatic children in association with comorbidities including sensitization to environmental allergens, clinical manifestations of atopy, food allergy and/or allergic rhinoconjunctivitis.[5] Besides Th2 cells also regulatory $CD4^+$ T cells (Tregs) expressing the TF FOXP3 are involved in the pathogenesis of childhood asthma, however the mechanisms are controversial.[6-10]

The origin of asthma is influenced by environmental, epigenetic and genetic factors. Thus, children living in microbe-rich environments, have lower risk for development of asthma and allergy.[11] Furthermore, analysis of DNA methylation revealed that paediatric asthmatics display hypomethylation of Th2 associated genes, including *IL-13*, *IL-4* and the T cell associated molecule *TIGIT*.[12] Genome-wide association study (GWAS) revealed single-nucleotide polymorphisms (SNPs) in several genetic loci including the TF Interferon Regulatory Factor 1 (IRF1) in childhood asthma.[6,13] Consistent with regulating Th1 versus Th2, Th9 and Tregs[14-18] differentiation as well as myeloid cell driven inflammation[19,20], *IRF1* SNPs associate with allergy and childhood AA[21,22] involving regulation of pro-inflammatory genes[23].

To identify the T-cell phenotypes and compositional changes associating with AA in childhood, we applied a 42-antibody mass cytometry panel in combination with unsupervised

computational analyses and manual gating in a group of well-characterized treatment-naïve children with AA and healthy (HC) from the CLARA/CLAUS study.[8,23-25] Deep profiling of T-cell phenotypes combined with bioinformatic analyses of the high-dimensional data resulted in an identification of a T-cell profile in childhood AA, which was related to the disease course and clinical parameters. The key features of childhood AA related T-cell aberrations are (i) lower frequency of memory $CD8^+$ T cells, (ii) overrepresented $TIGIT^+ICOS^+$ Th2 cells connected to eosinophilia and (iii) changes within Tregs characterized by an enrichment of naïve/resting Tregs and dysregulated effector (e)Tregs. The altered Treg compartment was linked to a lung function and memory $CD8^+$ T cells and, on the other hand, to eosinophilia via $TIGIT^+ICOS^+$Th2 cells. These data provide new insights that improve our understanding of childhood AA pathophysiology, and thereby guide new opportunities for disease monitoring and potentially therapy decision.

Materials and methods

Study Population.

This study analyzed data of N=23 (N=14 allergic asthmatic, N=9 healthy) children (Table S1,S3,S4) of the cross-sectional CLARA/CLAUS cohort, comprising N=273/361 4-15-year-old children with mild-to-moderate asthma and healthy controls, that were recruited since 01/2009 in the LMU children´s hospital.[8,24,25] Children were selected based on complete epidemiological data, treatment naivety, availability of IRF1 genotyping and cell availability for CyTOF. Allergic asthmatics were phenotyped based on a doctor´s diagnosis of asthma following the GINA-Guidelines[26], classical asthma symptoms, treatment-naivety in terms of asthma medication and a lung function indicating a significant reversible airflow obstruction (ATS/ERS guidelines)[27] and specific IgE-levels $\geq$ 0.35 IU/mL to at least one of 30 common aero- and food-allergens. Allergic comorbidity was defined as additional presence of atopic

dermatitis (AD), food allergy or allergic rhinitis. The course of disease was described as stable or with intermittent symptoms according to GINA guidelines[26]. Exclusion criteria included other chronic diseases, prematurity and infections, fever or use of steroids in the last 14 days before inclusion. Healthy controls had no pulmonary diseases including asthma, no allergic symptoms and were recruited in the LMU children´s hospital prior to outpatient daily procedures (e.g. fracture, hernia operation). Detailed questionnaires on general health, socioeconomic status and written informed consent was answered and obtained from the parents. Ethical approval was obtained by the local ethics board, LMU Munich, Germany (Nr. 379-08).

Cell staining and mass cytometry acquisition

PBMCs were isolated from Na-Heparin blood within 24h after blood withdrawal by Ficoll density gradient centrifugation, resuspended in freezing medium and stored in liquid nitrogen. For CyTOF experiment, samples were thawed, stained, barcoded and analysed in one batch in a Helios mass cytometer (Fluidigm) as described before[28].

Mass cytometry data analysis

Raw mass cytometry data were converted to Flow Cytometry Standard (FCS) 3.0 files during acquisition. Data normalization, compensation and processing for further analysis were done as previously described[28]. From each of the resulting individual samples, single, live, $CD45^+$ PBMC were gated in OMIQ according to ^{103}Rh-mDOTA for dead cell exclusion, DNA and event length parameters and CD45 expression (Figure S1). FlowSOM[29] clustering and subsequent meta-clustering, data visualization and opt-SNE plots[30] were performed in OMIQ. Data plotting and statistical analysis was performed using GraphPad Prism version 8.1.1. Heatmaps, principal component analysis and ROC curves were plotted with RStudio (Version 1.4.1103, packages gplots v3.1.0, factoextra, pROC).

Additional methods can be found in the Supplementary Material.

Results

Decreased total and central memory $CD8^+$ T cell frequency in children with AA.

We collected peripheral blood mononuclear cells (PBMC) from 23 children at the age from four to fifteen years, among them 14 suffering from allergic asthma (AA), which were treatment naïve and 9 healthy controls (HC) (Table S1). For the "Cytometry by Time of Flight" (CyTOF) analysis, frozen PBMC were thawed, barcoded and stained using a 42-antibody panel to identify T-cell populations as well as their activation and differentiation status based on the expression of lineage-specific markers, chemokine receptors and transcription factors (Table S2**)**. The analysis workflow integrated manual gating, computational analysis and statistical association of the extracted T-cell features with clinical parameters (Figure S1, Table S1-S4). After gating on the intact, live, single cells, we applied a t-distributed stochastic neighbour embedding (tSNE) integrating the information from 12 lineage-markers to classify the major cell populations within PBMC. Based on the tSNE representation we identified and manually gated seven distinct major cell populations (Figures 1A,B,S2A,B): $CD3^+CD8^+$ ($CD8^+$ T), $CD3^+CD4^+$ ($CD4^+$ T), $CD3^+CD4^+CD45RA^-CD25^+FOXP3^+$ (effector (e)Treg), $CD56^+CD16^+$ (NK), $CD3^+CD56^+$ (NKT), $CD3^+CD161^+TCRV\alpha7.2^+$ (MAIT), $CD3^+TCR\gamma\delta^+$ ($\gamma\delta$T) cells, for downstream evaluation. Analysis of the distribution of the detected T- and NK-cell populations in each individual and comparison of the frequency revealed that $CD8^+$ T-cell abundance was significantly changed in AA (Figure 1C,D).

Since the frequency of total $CD8^+$ T cells was lower in AA vs HC, we sought to understand which subpopulation best described this difference. For this, we subdivided $CD8^+$ T cells into naïve, central memory (CM), effector memory (EM) and EM cells (re-)expressing

CD45RA (TEMRA) based on the expression of CD45RA and CCR7 by manual gating (Figure 1E). There was a significantly lower frequency of CM and a similar trend for EM cells in AA versus HC (Figure 1F). Because $CD8^+$ T cells were previously associated with lung function in adult asthma[31], we correlated the ratio of total $CD8^+$ T cells to CM and EM frequencies of AA children with lung function as measured by percent-predicted ratio of forced expiratory volume in 1 sec to vital capacity (FEV1/VC). We observed a non-significant tendency for EM cells (Figure S3A), indicating that a $CD8^+$ T-cell association with lung function decline is a feature of adult asthma. However, the $CD8^+$ T-cell dysbalance occurs already in the childhood and is an early immunological phenomenon.

FlowSOM clustering was applied to further characterize $CD8^+$ T cells.[29] We computed 30 clusters (Figure S3B,C), of which only cluster c10 with a $CD127^+CD45RA^-$ memory phenotype was significantly downregulated in AA (Figure S3D-F). Cluster c10 expressed CD28 and high levels of the chemokine receptor CXCR3, suggesting a preserved capacity to proliferate[32], and to migrate to sites of inflammation[33].

These data reveal a $CD8^+$ T-cell dysbalance in AA children, characterized by underrepresented memory cells.

Elevated frequency of a novel $TIGIT^+ICOS^+$Th2-cell cluster in children with AA.

Consistent with the decreased $CD8^+$ T-cell abundance, the $CD4^+/CD8^+$ T-cell ratio was elevated in AA vs HC and positively correlated with blood eosinophil frequencies, a determinant of AA severity[34,35], which was also enhanced in AA of our cohort (Figure 2A-C).

$CD4^+$ T cells are considered as main regulators in type 2 asthma and eosinophilia[1-3,5,6]. To address potential disease-associated changes within $CD4^+$ T cells, we computed 30 $CD4^+$ T cell FlowSOM clusters (Figures 2D, S4A,B), of which c6 and c30 were significantly expanded

in AA vs HC children (Figures 2E). The heat map visualisation of the 30 markers mean-expression levels revealed that the significantly regulated clusters belonged to different clades, indicating specific phenotypic profile and function (Figure 2F).

Based on the highest expression of the Th2-specific TF GATA3[36] as well as the Th2-specific chemokine receptors CRTH2 and CCR4[37,38], cluster c6 and the neighbouring cluster c1 represented Th2-cells (Figure 2F,G). Cluster c6 differed from c1 by unique co-expression of TIGIT and ICOS. In the setting of malignant diseases and infection, TIGIT is a $CD8^+$ T-cell inhibitory molecule[39,40], while consistent with its hypomethylated state in childhood asthma[12], it enhances Th2 activation and Th2-driven allergic airway inflammation in the mouse model[41]. ICOS is required for IL-4 production and humoral immune responses in the mouse model of AA,[42] and accordingly enhances human Th2 responses[43]. The frequency of the $TIGIT^+ICOS^+$-expressing cluster c6, but not of c1, correlated with eosinophilia (Figure 2H, S4C,D), which specifically applied to children with additional presence of atopic dermatitis, food allergy or allergic rhinitis (Figure 2I), suggesting its involvement in AA associated with allergic comorbidities in connection with eosinophilia. Moreover, $TIGIT^+ICOS^+$ c6 cell frequencies positively correlated with the CD4/CD8 T-cell ratio in children with intermittent disease symptoms, while inversely in children with stable disease (Figure 2J), indicating its involvement in a more symptomatic AA.

The second $CD4^+$ T-cell cluster c30, is described in the Treg section below.

Summarizing, a $TIGIT^+ICOS^+$ Th2 cluster was enriched in children with AA, and associated with more symptomatic disease including allergic comorbidity linked to eosinophilia.

Altered ratio of the TIGIT$^+$ICOS$^+$ Th2 to Th1 cells in children with AA.

In childhood AA, the ratio between Th2 and Th1 cells is increased and low IFN-γ production during infancy is associated with an increased risk for allergy and asthma[44,45], and wheezing[46] development. To interrogate the Th2/Th1 balance in more detail, we analysed Th1 clusters and their relation to the TIGIT$^+$ICOS$^+$Th2 cells (c6). Based on the expression of the lineage specific TF T-BET[47], we identified 8 different Th1 clusters within CD4$^+$ T-cells, which were organized by hierarchical clustering into three different clades termed Th1-I, Th1-II, and Th1-III, showing distinct phenotypes (Figure 3A-C). They differed in the expression of CD127, the inhibitory receptors CTLA-4 and PD-1, as well as of ICOS, suggesting specific states of Th1-cell activation/dysfunction. The frequency of all clades was similar in AA vs HC (Figure 3D).

The ratio between the TIGIT$^+$ICOS$^+$ Th2 cluster and all T-BET$^+$ Th1 cells was increased in AA children vs HC, whereby clade Th1-II with the CD127$^+$ memory precursor phenotype[48], mainly contributed to this effect and was partially linked to eosinophilia (Figure 3E,F). Thus, in childhood AA TIGIT$^+$ICOS$^+$ Th2/Th1 ratio partly associated with eosinophilia.

Enrichment in circulating resting/naïve Tregs in children with AA.

The involvement of Tregs in childhood AA has been described, however without close characterization of Treg subpopulations.[7-10] Therefore, we next asked if the Treg composition is altered in paediatric AA. Among CD4$^+$ T-cells, the significantly enriched cluster c30 (Figure 2D,E), was visible as a distinct population in the t-SNE plot and expressed FOXP3, CD25, CD45RA, CCR7 and CD27 (Figure 4A) indicative of a naïve Treg phenotype.[49] Using manual gating (Figure S5), differential expression of FOXP3 and CD45RA permits sub-setting of FOXP3$^+$CD4$^+$ T cells into three main populations: fraction-I (Fr-I) CD45RA$^+$FOXP3^{low} resting/naïve Tregs, Fr-II CD45RA$^-$FOXP3^{high} eTregs and Fr-III CD45RA$^-$FOXP3^{low} cells,

which mostly are not bona fide Tregs.[49] We confirmed the location of cluster 30 within Treg Fr-I (Figure 4B,C), and also the overrepresentation of Fr-I in AA vs HC, while the abundance of Fr-II and Fr-III was similar in paediatric AA patients vs HC (Figure 4D). Manually gated $FOXP3^{+}CD25^{+}CD45RA^{-}$ eTregs matched with Fr-II, confirming the identification of eTregs by different gating strategies (Figure 4E). Consistent with the linear development model of Treg Fr-I towards Treg Fr-II[49], the abundance of Fr-I inversely correlated with Fr-II (Figure 4F). Moreover, there was a tendency for a negative correlation between the frequency of Fr-I and lung function as assessed by percent-predicted Tiffeneau index (FEV1/FVC) (Figure 4G). Finally, the abundance of Fr-I negatively correlated with the abundances of vs CM and EM $CD8^{+}$ T cells (Figure 4H).

Taken together, an overrepresentation of resting/naïve Tregs, inversely correlated with eTregs, suggesting an impaired eTregs differentiation in children with AA. The accumulating naïve/resting Tregs were linked to impaired lung function and negatively associated with memory $CD8^{+}$ T cells.

Altered $TIGIT^{+}ICOS^{+}$Th2/eTreg ratio associates with eosinophilia.

To better understand if the $FOXP3^{+}CD25^{+}CD45RA^{-}$ eTregs (Fr-II) compartment is qualitatively changed in childhood AA, FlowSOM was employed to identify and characterize two major clades within a total of 10 clusters (Figure 5A, S6A,B). Two clusters were underrepresented in children with AA, whereby c2 was more (>20% of total eTregs), and c10 less (<2% of total eTregs) abundant (Figure 5B,C). Cluster c10 was characterized by high IRF4, ICOS, CTLA-4 and CD28 expression indicating activated eTregs[49,50], while cluster c2 expressed all these molecules at average levels (Figure 5D). Considering the suggested impaired differentiation of eTregs and an overrepresentation of $TIGIT^{+}ICOS^{+}$Th2 cells in

childhood AA, we asked if the two phenomena were correlated, or were independent features of AA. In children with AA, the $TIGIT^+ICOS^+$ Th2/eTreg ratio was higher as compared to HC but failed to correlate with eosinophilia. In contrast, the $TIGIT^+ICOS^+$ Th2-cell ratio to eTreg_c2 and eTreg_c10, correlated significantly suggesting that their underrepresentation was statistically related to the $TIGIT^+ICOS^+$Th2 associated eosinophilia.

Integrated T cell signature distinguishes children with AA from HC.

To investigate if the T-cell signature obtained from our high-dimensional data analysis distinguishes AA from HC, we performed principal component analysis (PCA) based on frequencies of T-cell populations, clusters and ratios that were significantly changed in paediatric AA. The PCA of these parameters separated AA from HC children at the first principal component (PC1), indicating that the detected dysbalanced T-cell composition allows a discrimination between AA and HC (Figure 6A). The analysis of the contribution of 8 variables to the first two principal components revealed that the frequency of naïve/resting Tregs (CD4_c30), together with the CD4/CD8 ratio and $CD8^+$ T cell frequency were mainly driving this effect (Figure 6B). To further understand the association of the differentially regulated cluster abundances with the AA phenotype, we performed ROC analyses which revealed a relation of resting/naïve Tregs (CD4_c30), eTreg_c2 and eTreg_c10 to the childhood AA phenotype (sensitivity, true positive rate) (Figure 6C), further supporting the relevant involvement of the Treg dysbalance in childhood AA.

Finally, we tested whether the obtained T cell profiles were associated, and explainable by the presence of distinct *IRF1*-SNPs[21,23]. For this, we determined the presence of four *IRF1*-SNPs associating with childhood AA: rs10035166, rs2706384, rs2070721 and rs17622656[23]. A mutually adjusted risk score for *IRF1*-dependent asthma was calculated and correlated with the

abundance of all significantly altered T-cell populations. Among these, the *IRF1*-score inversely correlated with the frequency of $CD8^+$ T cells (Figure 6D) in HC, but remarkably not in children with AA. Considering that lower $CD8^+$ T-cell frequencies were associated with AA (Figure 1D), *IRF1*-SNPs might contribute to the AA-like perturbances in $CD8^+$ T-cell compartment already in health. However, in AA probably more prominent other genetic drivers impose the AA phenotype.

Discussion

Most adult cases of asthma begin in childhood and approximately 10% of children in the European Union and North America are affected, with the vast majority suffering from type 2 AA.[51] Our understanding of this disorder is complicated by the overlap of the disease with development and maturation of the immune system during childhood. Therefore, a deeper understanding of immunologic aberrations may serve as a framework to identify target-directed treatment options, and to guide the use of existing options to control AA in childhood.

To systematically analyse T-cell subpopulations associated with childhood AA, and their phenotypes we performed deep single-cell profiling of PBMCs by mass cytometry, which revealed a T-cell signature characterized by a lower frequency of memory $CD8^+$ T cells, increased abundance of $TIGIT^+ICOS^+$Th2 cells and naïve/resting Tregs as well as by disturbances within eTregs in comparison to HC.

While a mechanistic contribution of $CD8^+$ T cells to childhood AA is elusive, their involvement in adult asthma was already reported.[5,31,52] Our analysis revealed a significantly decreased frequency of total and in particular of memory $CD8^+$ T cells in children with AA, which only weekly associated with impaired lung function. Moreover, the abundance of $CXCR3^{high}$ memory $CD8^+$ T cells was reduced in the peripheral blood. Since CXCR3 directs

cell recruitment to sites of inflammation and consecutive bystander activation[33], the decrease in circulating memory $CD8^+$ T cells may reflect their enhanced recruitment to inflamed lung, where they may contribute to lung pathology over time. In line with that, the accumulation of $CD8^+$ T cells in the lung tissue is associated with lung function impairment in adult AA.[31] Thus, our data establish a disturbed peripheral $CD8^+$ T cell homeostasis as an early feature of AA.

An increased CD4/CD8 T-cell ratio has previously been described for asthma in young adults.[53] Our data extend this observation towards childhood AA and reveal its association with increased eosinophilia, which is linked to poorer asthma control.[34,35] Among $CD4^+$ T cells, a $TIGIT^+ICOS^+$Th2 cluster was significantly expanded in AA and correlated with eosinophilia, in particular in AA children with allergic comorbidities, suggesting its association with rather complex, polysymptomatic disease. Considering that PBMC for the analysis were obtained from treatment-naïve children, this result suggests that the correlation of $TIGIT^+ICOS^+$Th2 cells with the CD4/CD8 T-cell ratio may indicate subsequent poorer AA control.

A $TIGIT^+ICOS^+$Th2 population has not been detected in AA so far and could be specific for childhood, since a decreased *TIGIT* methylation status has been described only for childhood AA.[12] The ratio of $TIGIT^+ICOS^+$Th2 cells to Th1 cells and Th1-clades as well as to dysbalanced eTregs was higher in children with AA vs HC and associated partially with eosinophilia, suggesting the overriding contribution of this Th2 cluster to eosinophilic inflammation. Thus, the expansion of $TIGIT^+ICOS^+$Th2 cluster is an early immunological event, which contributes to an eosinophilic bias in paediatric AA.

Tregs in childhood asthma seem to play a critical role and different controversial reports describe qualitative or quantitative dysbalances or no alterations[7-10], however without closer examination of Treg phenotype/subpopulations. Our data show an accumulation of resting/naïve Tregs. Together with the inverse correlation with eTregs, this finding may indicate a block in the differentiation towards eTregs. The pathophysiological implication of

disturbances within the Treg compartment seems to involve following features of AA:(i) a declined lung function and an inverse correlation of naïve/resting Tregs to memory $CD8^+$ T cells and (ii) eosinophilia, which significantly associated with the $TIGIT^+ICOS^+$Th2 ratio to the two downregulated eTreg clusters (eTreg_c2 and eTreg_c10). Consistent with this notion, ROC analysis revealed that all differentially regulated Treg clusters CD4_c30 (Fr-I, naïve/resting Tregs), eTreg_c2 and eTreg_c10 associate with the phenotype and can be included as markers for a prediction model. Thus, we add a new level of complexity to the appreciated role of Tregs in AA revealing distinct regulation of specific Treg subsets including probable disturbance in the development of naïve towards eTregs and demonstrating their involvement in disease pathophysiology. Therefore, our results may help to reconcile the previous inconsistency regarding the role of Tregs in childhood AA.

Integration of the significantly regulated T-cell populations and ratios, allowed a clear separation of children with AA from HC, indicating that the described T-cell signature associates with the disease phenotype and can be used for further mechanistic and biomarker analysis including bigger cohorts. Mechanistically, our analysis revealed an association of *IRF1*-SNPs with $CD8^+$ T-cell frequencies in health but not in disease, suggesting a partial IRF1-contribution to the $CD8^+$ T-cell dysbalance, which could be overruled by a prevailing involvement of other main genetic drivers.[13]

Summarizing, our results have implications for our understanding of the involvement of T-cell subpopulations in childhood AA, including the pathophysiology considering the aberrances in the Treg compartment, for immune monitoring using the described perturbances and probably for the disease course prediction based on the presence of $TIGIT^+ICOS^+$ Th2 cells. The majority of the described AA-associated aberrations including $CD8^+$ T cells, $TIGIT^+ICOS^+$ Th2 cells and eTregs were detected in non-naïve compartment indicating an already fixed immunological imprinting. This implies a need for an early diagnosis to pre-empt the

establishment of these disturbances and for treatment options to consider the non-naïve nature of the T-cell aberrations.

Author contributions

The study was designed and analyses were guided by MH with the input of HEM and BS. JT, AB and BS recruited the donors and their clinical information, collected the blood samples and organized the sampling. Mass cytometry was conducted by ARS at the DRFZ Berlin. HR, ARS, AR, AB, JT, BS and HEM analyzed data and made the figures. HDC, WB and BTS analyzed the data. HR, HEM, BS and MH prepared the manuscript.

Conflict of interest

All other authors declare no commercial or financial conflict of interest. BS reports grants from DFG, grants from EU, during the conduct of the study; grants from DFG, personal fees from consultancy, outside the submitted work.

References

1. Brusselle GG, Maes T, Bracke KR. Eosinophils in the spotlight: Eosinophilic airway inflammation in nonallergic asthma. *Nat Med* **19**, 977-979 (2013).

2. Wenzel SE. Asthma phenotypes: the evolution from clinical to molecular approaches. *Nat Med* **18**, 716-725 (2012).

3. Barnes PJ. Targeting cytokines to treat asthma and chronic obstructive pulmonary disease. *Nat Rev Immunol* **18**, 454-466 (2018).

4. Fallon PG, Schwartz C. The high and lows of type 2 asthma and mouse models. *J Allergy Clin Immunol* **145**, 496-498 (2020).

5. Holgate ST, Wenzel S, Postma DS, Weiss ST, Renz H, Sly PD. Asthma. *Nat Rev Dis Primers* **1**, 15025 (2015).

6. Krusche J, Basse S, Schaub B. Role of early life immune regulation in asthma development. *Semin Immunopathol* **42**, 29-42 (2020).

7. Lee JH, Yu HH, Wang LC, Yang YH, Lin YT, Chiang BL. The levels of CD4+CD25+ regulatory T cells in paediatric patients with allergic rhinitis and bronchial asthma. *Clin Exp Immunol* **148**, 53-63 (2007).

8. Raedler D, Ballenberger N, Klucker E, *et al.* Identification of novel immune phenotypes for allergic and nonallergic childhood asthma. *J Allergy Clin Immunol* **135**, 81-91 (2015).

9. Schroder PC, Illi S, Casaca VI, *et al.* A switch in regulatory T cells through farm exposure during immune maturation in childhood. *Allergy* **72**, 604-615 (2017).

10. Hartl D, Koller B, Mehlhorn AT, *et al.* Quantitative and functional impairment of pulmonary CD4+CD25hi regulatory T cells in pediatric asthma. *J Allergy Clin Immunol* **119**, 1258-1266 (2007).

11. von Mutius E, Vercelli D. Farm living: effects on childhood asthma and allergy. *Nat Rev Immunol* **10**, 861-868 (2010).

12. Yang IV, Pedersen BS, Liu A, *et al.* DNA methylation and childhood asthma in the inner city. *J Allergy Clin Immunol* **136**, 69-80 (2015).

13. Kabesch M, Tost J. Recent findings in the genetics and epigenetics of asthma and allergy. *Semin Immunopathol* **42**, 43-60 (2020).

14. Kano S, Sato K, Morishita Y, *et al.* The contribution of transcription factor IRF1 to the interferon-gamma-interleukin 12 signaling axis and TH1 versus TH-17 differentiation of CD4+ T cells. *Nat Immunol* **9**, 34-41 (2008).

15. McElligott DL, Phillips JA, Stillman CA, Koch RJ, Mosier DE, Hobbs MV. CD4+ T cells from IRF-1-deficient mice exhibit altered patterns of cytokine expression and cell subset homeostasis. *J Immunol* **159**, 4180-4186 (1997).

16. Elser B, Lohoff M, Kock S, *et al.* IFN-gamma represses IL-4 expression via IRF-1 and IRF-2. *Immunity* **17**, 703-712 (2002).

17. Campos Carrascosa L, Klein M, Kitagawa Y, *et al.* Reciprocal regulation of the Il9 locus by counteracting activities of transcription factors IRF1 and IRF4. *Nat Commun* **8**, 15366 (2017).

18. Fragale A, Gabriele L, Stellacci E, *et al.* IFN regulatory factor-1 negatively regulates CD4+ CD25+ regulatory T cell differentiation by repressing Foxp3 expression. *J Immunol* **181**, 1673-1682 (2008).

19. Lohoff M, Ferrick D, Mittrucker HW, *et al.* Interferon regulatory factor-1 is required for a T helper 1 immune response in vivo. *Immunity* **6**, 681-689 (1997).

20. Qiao Y, Giannopoulou EG, Chan CH, *et al.* Synergistic activation of inflammatory cytokine genes by interferon-gamma-induced chromatin remodeling and toll-like receptor signaling. *Immunity* **39**, 454-469 (2013).

21. Schedel M, Pinto LA, Schaub B, *et al.* IRF-1 gene variations influence IgE regulation and atopy. *Am J Respir Crit Care Med* **177**, 613-621 (2008).

22. Nakao F, Ihara K, Kusuhara K, *et al.* Association of IFN-gamma and IFN regulatory factor 1 polymorphisms with childhood atopic asthma. *J Allergy Clin Immunol* **107**, 499-504 (2001).

23. Landgraf-Rauf K, Boeck A, Siemens D, *et al.* IRF-1 SNPs influence the risk for childhood allergic asthma: A critical role for pro-inflammatory immune regulation. *Pediatr Allergy Immunol* **29**, 34-41 (2018).

24. Krusche J, Twardziok M, Rehbach K, *et al.* TNF-alpha-induced protein 3 is a key player in childhood asthma development and environment-mediated protection. *J Allergy Clin Immunol* **144**, 1684-1696 e1612 (2019).

25. Krautenbacher N, Flach N, Bock A, *et al.* A strategy for high-dimensional multivariable analysis classifies childhood asthma phenotypes from genetic, immunological, and environmental factors. *Allergy* **74**, 1364-1373 (2019).

26. Stone RG, McDonald M, Elnazir B. Global Initiative for Asthma 2019 Guidelines: New Changes to the Treatment of Mild Asthmatics 12 Years and Older. *Ir Med J* **113**, 69 (2020).

27. Beydon N, Davis SD, Lombardi E, *et al.* An official American Thoracic Society/European Respiratory Society statement: pulmonary function testing in preschool children. *Am J Respir Crit Care Med* **175**, 1304-1345 (2007).

28. Romero-Olmedo AJ, Schulz AR, Huber M, *et al.* Deep phenotypical characterization of human CD3(+) CD56(+) T cells by mass cytometry. *Eur J Immunol*, (2020).

29. Van Gassen S, Callebaut B, Van Helden MJ, *et al.* FlowSOM: Using self-organizing maps for visualization and interpretation of cytometry data. *Cytometry A* **87**, 636-645 (2015).

30. Amir el AD, Davis KL, Tadmor MD, *et al.* viSNE enables visualization of high dimensional single-cell data and reveals phenotypic heterogeneity of leukemia. *Nat Biotechnol* **31**, 545-552 (2013).

31. den Otter I, Willems LN, van Schadewijk A, *et al.* Lung function decline in asthma patients with elevated bronchial CD8, CD4 and CD3 cells. *Eur Respir J* **48**, 393-402 (2016).

32. Topp MS, Riddell SR, Akatsuka Y, Jensen MC, Blattman JN, Greenberg PD. Restoration of CD28 expression in CD28- CD8+ memory effector T cells reconstitutes antigen-induced IL-2 production. *J Exp Med* **198**, 947-955 (2003).

33. Maurice NJ, McElrath MJ, Andersen-Nissen E, Frahm N, Prlic M. CXCR3 enables recruitment and site-specific bystander activation of memory CD8(+) T cells. *Nat Commun* **10**, 4987 (2019).

34. Price DB, Rigazio A, Campbell JD, *et al.* Blood eosinophil count and prospective annual asthma disease burden: a UK cohort study. *Lancet Respir Med* **3**, 849-858 (2015).

35. Bousquet J, Chanez P, Lacoste JY, *et al.* Eosinophilic inflammation in asthma. *N Engl J Med* **323**, 1033-1039 (1990).

36. Nakayama T, Hirahara K, Onodera A, *et al.* Th2 Cells in Health and Disease. *Annu Rev Immunol* **35**, 53-84 (2017).

37. Cosmi L, Annunziato F, Galli MIG, Maggi RME, Nagata K, Romagnani S. CRTH2 is the most reliable marker for the detection of circulating human type 2 Th and type 2 T cytotoxic cells in health and disease. *Eur J Immunol* **30**, 2972-2979 (2000).

38. Bonecchi R, Bianchi G, Bordignon PP, *et al.* Differential expression of chemokine receptors and chemotactic responsiveness of type 1 T helper cells (Th1s) and Th2s. *J Exp Med* **187**, 129-134 (1998).

39. Manieri NA, Chiang EY, Grogan JL. TIGIT: A Key Inhibitor of the Cancer Immunity Cycle. *Trends Immunol* **38**, 20-28 (2017).

40. Schorer M, Rakebrandt N, Lambert K, *et al.* TIGIT limits immune pathology during viral infections. *Nat Commun* **11**, 1288 (2020).

41. Kourepini E, Paschalidis N, Simoes DC, Aggelakopoulou M, Grogan JL, Panoutsakopoulou V. TIGIT Enhances Antigen-Specific Th2 Recall Responses and Allergic Disease. *J Immunol* **196**, 3570-3580 (2016).

42. Dong C, Juedes AE, Temann UA, *et al.* ICOS co-stimulatory receptor is essential for T-cell activation and function. *Nature* **409**, 97-101 (2001).

43. Wassink L, Vieira PL, Smits HH, *et al.* ICOS expression by activated human Th cells is enhanced by IL-12 and IL-23: increased ICOS expression enhances the effector function of both Th1 and Th2 cells. *J Immunol* **173**, 1779-1786 (2004).

44. Wright AL. The epidemiology of the atopic child: who is at risk for what? *J Allergy Clin Immunol* **113**, S2-7 (2004).

45. Vuillermin PJ, Ponsonby AL, Saffery R, *et al.* Microbial exposure, interferon gamma gene demethylation in naive T-cells, and the risk of allergic disease. *Allergy* **64**, 348-353 (2009).

46. Stern DA, Guerra S, Halonen M, Wright AL, Martinez FD. Low IFN-gamma production in the first year of life as a predictor of wheeze during childhood. *J Allergy Clin Immunol* **120**, 835-841 (2007).

47. Huber M, Lohoff M. IRF4 at the crossroads of effector T-cell fate decision. *Eur J Immunol* **44**, 1886-1895 (2014).

48. Kaech SM, Tan JT, Wherry EJ, Konieczny BT, Surh CD, Ahmed R. Selective expression of the interleukin 7 receptor identifies effector CD8 T cells that give rise to long-lived memory cells. *Nat Immunol* **4**, 1191-1198 (2003).

49. Sakaguchi S, Mikami N, Wing JB, Tanaka A, Ichiyama K, Ohkura N. Regulatory T Cells and Human Disease. *Annu Rev Immunol* **38**, 541-566 (2020).

50. Zheng Y, Chaudhry A, Kas A, *et al.* Regulatory T-cell suppressor program co-opts transcription factor IRF4 to control T(H)2 responses. *Nature* **458**, 351-356 (2009).

51. Papadopoulos NG, Custovic A, Cabana MD, *et al.* Pediatric asthma: An unmet need for more effective, focused treatments. *Pediatr Allergy Immunol* **30**, 7-16 (2019).

52. van Rensen EL, Sont JK, Evertse CE, *et al.* Bronchial CD8 cell infiltrate and lung function decline in asthma. *Am J Respir Crit Care Med* **172**, 837-841 (2005).

53. Lu Y, Kared H, Tan SW, *et al.* Dynamics of helper CD4 T cells during acute and stable allergic asthma. *Mucosal Immunol* **11**, 1640-1652 (2018).

Figure 1. Decreased total and central memory $CD8^+$ T cell frequency in children with AA. **A.** To the left t-distributed stochastic neighbour embedding (tSNE) plot on concatenated live cells from all 23 samples with manually gated main T-cell populations and NK cells based on the expression of individual molecules depicted in the tSNE plots in **B**. To the right, heat map of color coded z-scores of the mean marker expression values after row normalization. **B.** tSNE visualization of indicated marker expression of concatenated all files. **C.** Distribution of main T-cell populations and NK cells in each individual (AA n=14 and HC n=9). **D**. Comparison of main populations between AA and HC samples (mean ± SD, *P* value by Mann-Whitney test). **E.** Dot plot shows gating strategy on concatenated all files to identify $CD8^+$ T central memory (CM, $CCR7^+CD45RA^-$), effector memory (EM, $CCR7^-CD45RA^-$), TEMRA ($CCR7^-CD45RA^+$) and naïve ($CCR7^+CD45RA^+$) cells **F.** Scatter bar graphs represent the frequency in each sample for the indicated $CD8^+$ T-cell subpopulation (mean, *P* value by Mann-Whitney test).

Figure 2. Elevated frequency of a novel $TIGIT^+ICOS^+$ Th2-cell cluster in children with AA A. Comparison of CD4/CD8 T-cell ratio in HC and AA samples (mean, *P* value by Mann-Whitney test). **B**. Linear regression analysis of CD4/CD8 T-cell ratio versus blood eosinophil frequency in children with AA. Each dot represents one individual. **C**. Scatter bar graph represents the eosinophil frequency in each sample (mean, *P* value by Mann-Whitney test). **D.** tSNE visualization of 30 FlowSOM clusters in $CD4^+$ T-cell population (left) and of clusters c6, and c30 (to the right). The plots display concatenated all samples. **E.** Scatter bar graphs represent the cluster frequency in each sample for c6 and c30 (mean, *P* value by Mann-Whitney test). **F.** Heat map of color coded z-scores of the mean marker expression values after row normalization. **G.** Histograms display the mean expression of depicted markers by the cluster c6 (dark blue), c1 (light blue) and all other clusters (black) of concatenated all samples. **H.** Linear regression analysis of c6($TIGIT^+ICOS^+$) cluster frequency within $CD4^+$ T cells versus

blood eosinophil frequency. Each dot represents one individual. **I.** Linear regression analysis of c6($TIGT^+ICOS^+$) cluster frequency versus eosinophil frequency in children with AA. Left graph depicts the samples from AA children with comorbidity (at least one allergic comorbidity), right graph without comorbidity. Each dot represents one individual. **J.** Linear regression analysis of CD4/CD8 T-cell ratio versus c6($TIGT^+ICOS^+$) cluster frequency. Left graph depicts AA children with intermittent symptoms, right graph with a stable disease. Each dot represents one individual.

Figure 3. Altered ratio of the $TIGIT^+ICOS^+$ Th2 cluster to Th1 cells in children with AA. **A.** Heat map of color coded z-scores of the mean marker expression values after column normalization. Indicated are three clades of Th1 cells: Th1-I (c26 and c28), Th1-II (c21, c22 and c8) and Th1-III (c27, c19 and c18). Th1 cluster were selected from Figure 2F based on the T-BET positivity. **B.** Overlay tSNE plots of CD127, CTLA4, PD1 and ICOS expression for clades Th1-I-III, shown in heat map in A. The cells of concatenated all samples are shown. **C.** tSNE visualization of Th1 clades within $CD4^+$ T cells: Th1-I (light blue), Th1-II (red) and Th1-III (purple). **D.** Scatter bar graphs show the respective Th1 clade frequency in each sample, (mean, *P* value by Mann-Whitney test). **E.** Scatter bar graphs represent the respective c6($TIGIT^+ICOS^+$)/ Th1 or Th1-clade ratios (mean, *P* value by Mann-Whitney test). **F.** Linear regression analysis of the c6($TIGIT^+ICOS^+$)/ Th1 ratio versus blood eosinophil frequency in children with AA. Each dot represents one individual.

Figure 4. Increased frequency of resting/naïve Tregs in children with AA. A. Expression of the indicated molecules visualized in the tSNE plots by total $CD4^+$ T cells (all samples concatenated), spatial location of $CD4^+$ T-cell cluster c30 is highlighted by red circle. **B.**

Representative example of the gating strategy to identify Treg fractions (Fr)-I-III. **C.** Dot plot of concatenated all samples with an overlay of $CD4^+$ T-cell cluster c30. **D**. Scatter bar graphs represent the frequency of indicated Treg fractions in each sample (mean, *P* value by Mann-Whitney test). **E.** tSNE visualization of $CD4^+$ T cells and eTregs of concatenated all files (left) and manually gated Treg Fr-I (middle) and Fr–II (right). **F.** Linear regression analysis of Treg-Fr-II versus Treg-Fr-I in children with AA. Each dot represents one individual. **G**. Linear regression analysis of CD4_c30 versus Tiffenau index forced expiratory volume in 1s vs forced vital capacity (FEV1/FVC, % of predicted) in children with AA. Each dot represents one individual. **H.** Linear regression analysis of the CM and EM $CD8^+$ T cells versus Treg-Fr-I in children with AA. Each dot represents one individual.

Figure 5. Significantly regulated Treg clusters associate with the AA phenotype. A. Heat map of color coded z-scores of the mean marker expression values normalized per column of ten FlowSOM based eTreg clusters. **B.** tSNE visualization of FlowSOM eTreg clusters c2 (red), c10 (blue) and background (grey) of concatenated all samples. **C.** Scatter bar graph represents the frequency in each sample for eTreg clusters c2 and c10 (mean, *P* value by Mann-Whitney test). **D.** Histograms display the mean expression of depicted markers by the cluster c2 (red), c10 (blue) and all other clusters (black). **E.** Scatter bar graph represents the frequency in each sample for the c6($TIGIT^+ICOS^+$)/eTreg ratio (mean, *P* value by Mann-Whitney test). **F.** Linear regression analysis of the respective ratios versus blood eosinophil frequency in children with AA. Each dot represents one individual.

Figure 6. Integrated T cell signature distinguishes children with AA from HC. A. Principal component analysis (PCA) of the 14 AA and 9 HC samples based on the significantly regulated

subpopulations ($CD8^+$ T cells, CM $CD8^+$ T cells, $CD8^+$ T-cell_c10, $CD4^+$ T-cell_c6, $CD4^+$ T-cell_c30, eTreg_c2, eTreg_c10 and CD4/CD8 T-cell ratio). AA are shown in red, HC in blue. **B.** Correlation circle represents the contributions of the subpopulations to the variability. **C.** Receiver operating characteristic (ROC) curves were calculated for $CD4^+$ T cell cluster c30 (CD4_c30), eTreg cluster c2 (eTreg_c2) and eTreg c10 (eTreg_c10) in AA vs HC. **D.** Linear regression analysis of $CD8^+$ T cells for children with AA (left), HC (middle) and for all samples (right) versus IRF1 risk score. Each dot represents one individual.

FIGURE 1

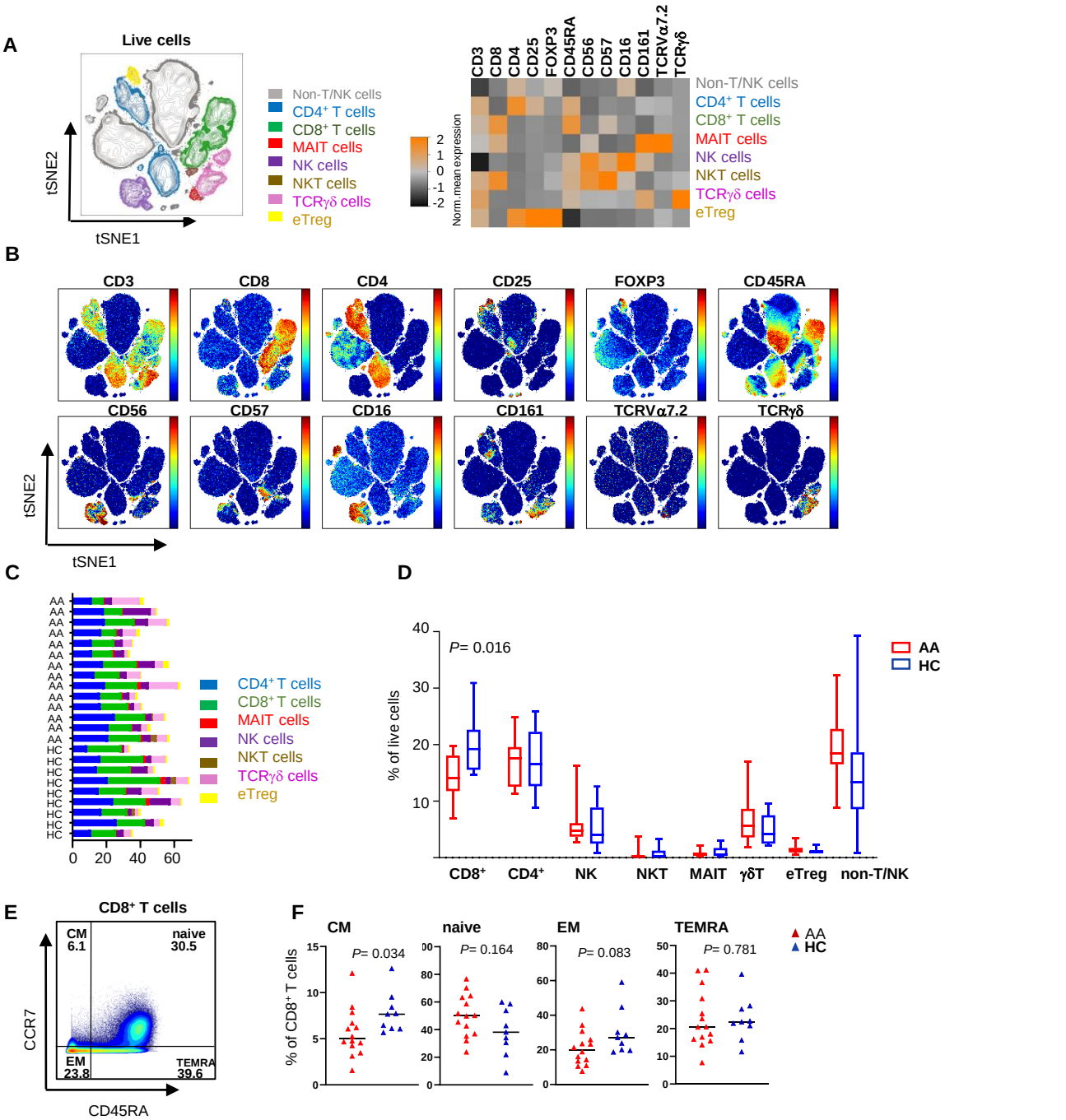
A
Live cells
tSNE2
tSNE1
Non-T/NK cells
CD4+ T cells
CD8+ T cells
MAIT cells
NK cells
NKT cells
TCRγδ cells
eTreg
CD3 CD8 CD4 CD25 FOXP3 CD45RA CD56 CD57 CD16 CD161 TCRVα7.2 TCRγδ
Norm.mean expression
2 1 0 -1 -2
B
CD3 CD8 CD4 CD25 FOXP3 CD45RA
CD56 CD57 CD16 CD161 TCRVα7.2 TCRγδ
tSNE2
tSNE1
C
AA
HC
0 20 40 60
CD4+ T cells
CD8+ T cells
MAIT cells
NK cells
NKT cells
TCRγδ cells
eTreg
D
P= 0.016
% of live cells
AA
HC
CD8+ CD4+ NK NKT MAIT γδT eTreg non-T/NK
E
CD8+ T cells
CM 6.1
naive 30.5
EM 23.8
TEMRA 39.6
CCR7
CD45RA
F
CM
naive
EM
TEMRA
P= 0.034
P= 0.164
P= 0.083
P= 0.781
% of CD8+ T cells
AA
HC

FIGURE 2

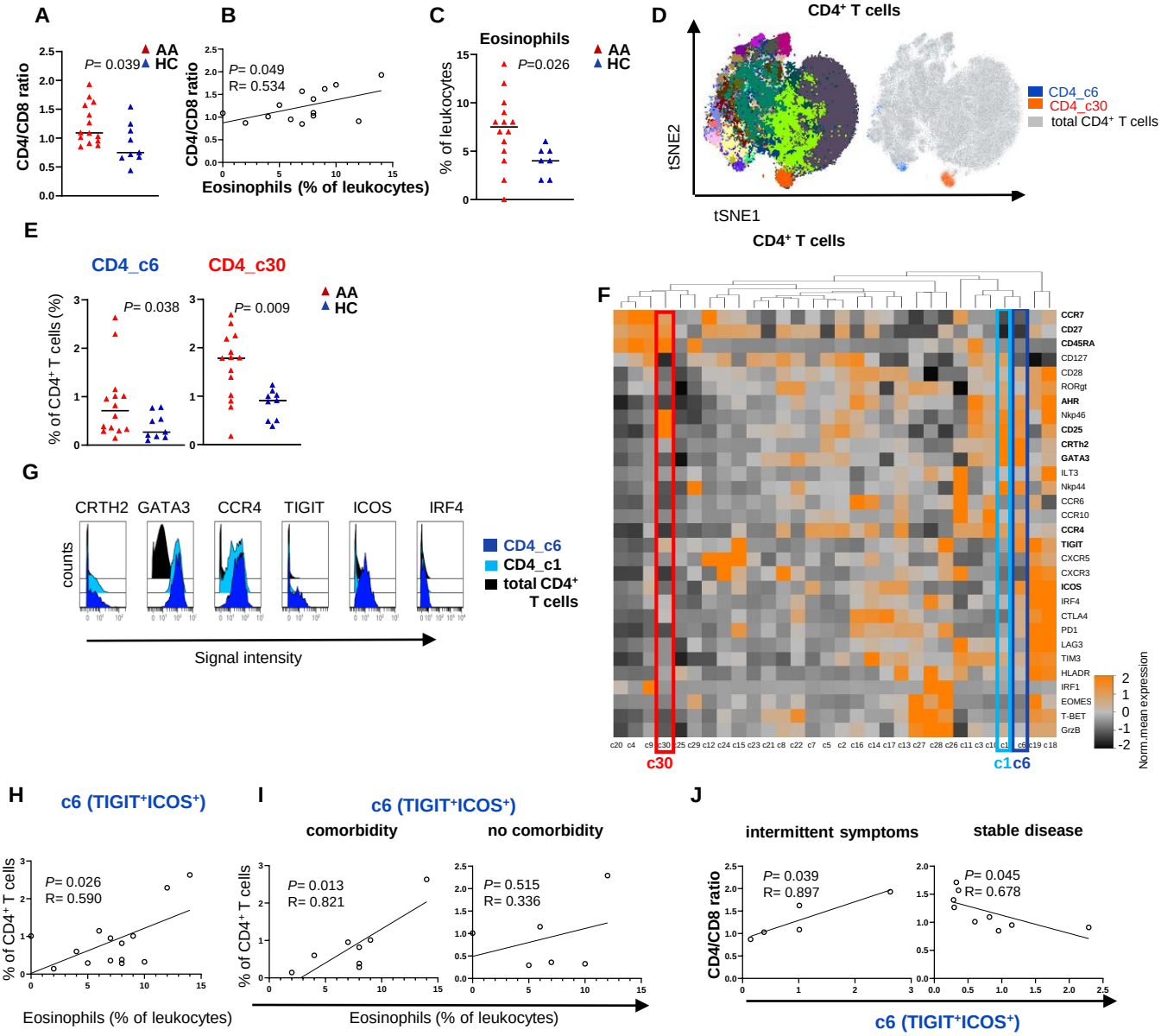
A
CD4/CD8 ratio
P= 0.039
AA
HC
B
CD4/CD8 ratio
P= 0.049
R= 0.534
Eosinophils (% of leukocytes)
C
Eosinophils
P=0.026
AA
HC
% of leukocytes
D
CD4+ T cells
CD4_c6
CD4_c30
total CD4+ T cells
tSNE2
tSNE1
E
CD4_c6
CD4_c30
P= 0.038
P= 0.009
AA
HC
% of CD4+ T cells (%)
F
CD4+ T cells
CCR7
CD27
CD45RA
CD127
CD28
RORgt
AHR
Nkp46
CD25
CRTh2
GATA3
ILT3
Nkp44
CCR6
CCR10
CCR4
TIGIT
CXCR5
CXCR3
ICOS
IRF4
CTLA4
PD1
LAG3
TIM3
HLADR
IRF1
EOMES
T-BET
GrzB
Norm.mean expression
c30
c1 c6
G
CRTH2
GATA3
CCR4
TIGIT
ICOS
IRF4
counts
CD4_c6
CD4_c1
total CD4+ T cells
Signal intensity

H
c6 (TIGIT+ICOS+)
P= 0.026
R= 0.590
% of CD4+ T cells
Eosinophils (% of leukocytes)
I
c6 (TIGIT+ICOS+)
comorbidity
no comorbidity
P= 0.013
R= 0.821
P= 0.515
R= 0.336
% of CD4+ T cells
Eosinophils (% of leukocytes)
J
intermittent symptoms
stable disease
P= 0.039
R= 0.897
P= 0.045
R= 0.678
CD4/CD8 ratio
c6 (TIGIT+ICOS+)

FIGURE 3

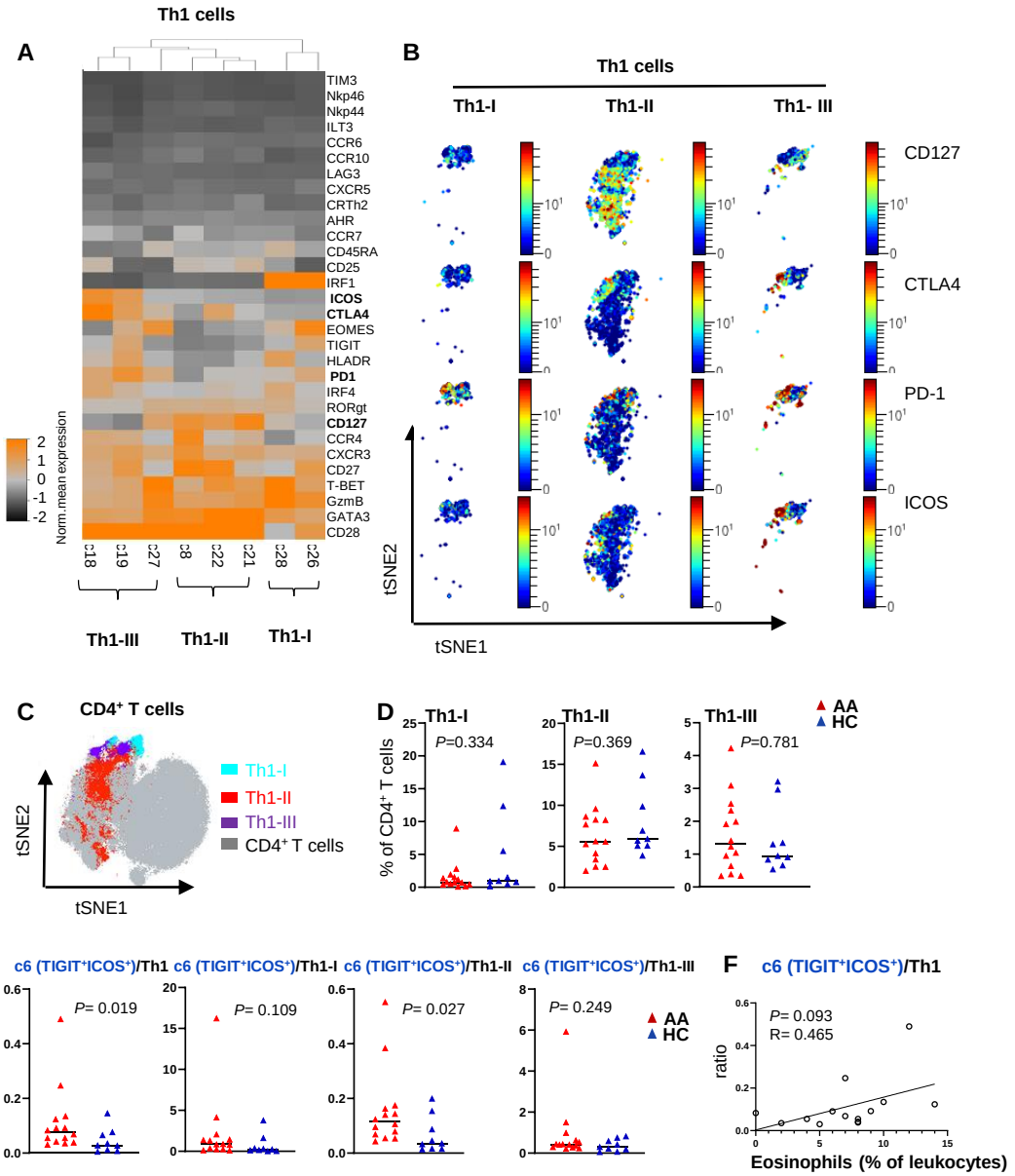
Th1 cells
A
TIM3
Nkp46
Nkp44
ILT3
CCR6
CCR10
LAG3
CXCR5
CRTh2
AHR
CCR7
CD45RA
CD25
IRF1
ICOS
CTLA4
EOMES
TIGIT
HLADR
PD1
IRF4
RORgt
CD127
CCR4
CXCR3
CD27
T-BET
GzmB
GATA3
CD28
Norm.mean expression
2
1
0
-1
-2
C18
C19
C27
C8
C22
C21
C28
C26
Th1-III
Th1-II
Th1-I
B
Th1 cells
Th1-I
Th1-II
Th1- III
CD127
CTLA4
PD-1
ICOS
tSNE2
tSNE1
C
CD4⁺ T cells
tSNE2
tSNE1
Th1-I
Th1-II
Th1-III
CD4⁺ T cells
D
Th1-I
Th1-II
Th1-III
AA
HC
P=0.334
P=0.369
P=0.781
% of CD4⁺ T cells
E
c6 (TIGIT⁺ICOS⁺)/Th1
c6 (TIGIT⁺ICOS⁺)/Th1-I
c6 (TIGIT⁺ICOS⁺)/Th1-II
c6 (TIGIT⁺ICOS⁺)/Th1-III
P= 0.019
P= 0.109
P= 0.027
P= 0.249
AA
HC
ratio
F
c6 (TIGIT⁺ICOS⁺)/Th1
P= 0.093
R= 0.465
ratio
Eosinophils (% of leukocytes)

FIGURE 4

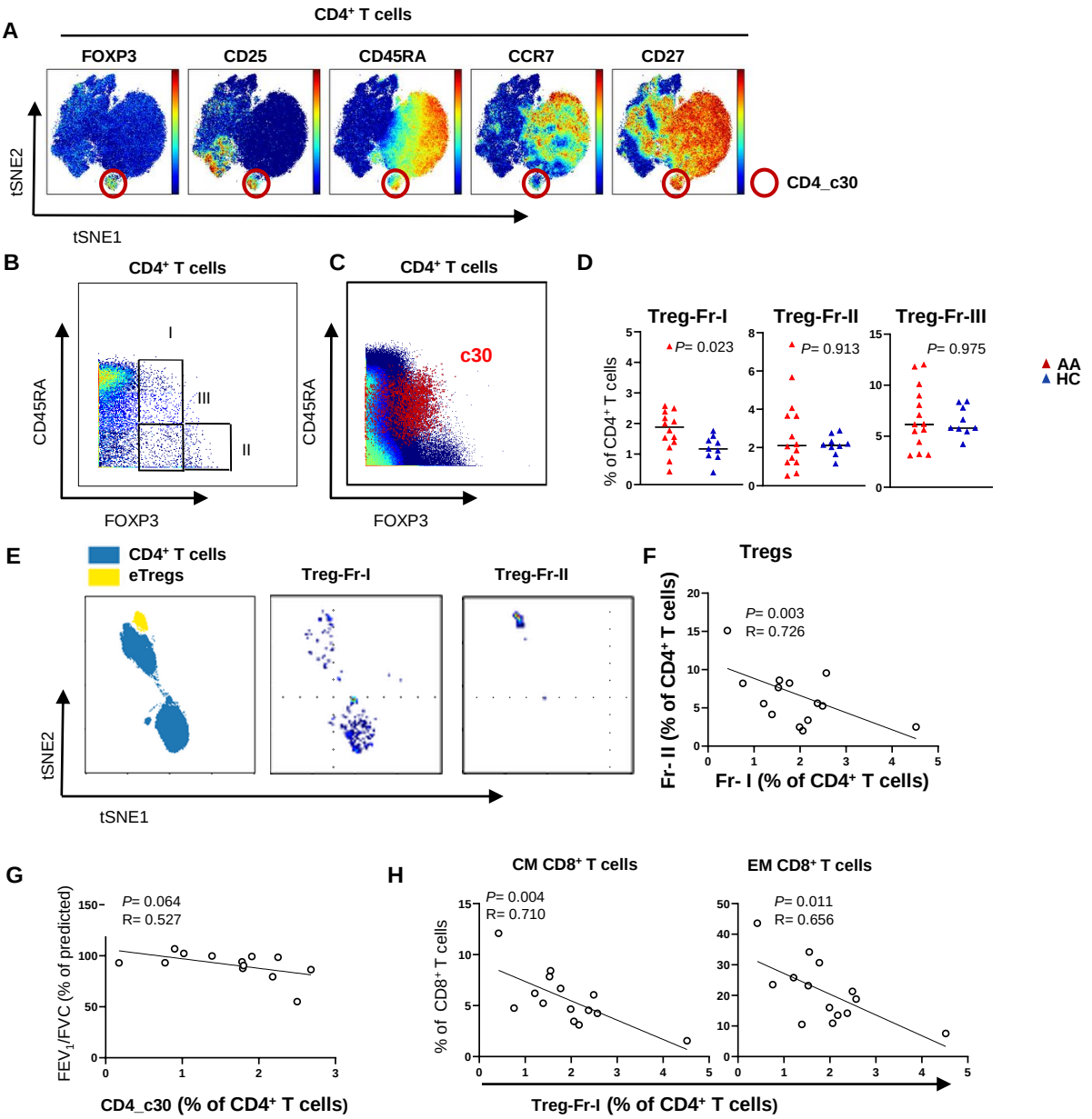
A
CD4⁺ T cells
FOXP3
CD25
CD45RA
CCR7
CD27
tSNE2
tSNE1
CD4_c30
B
CD4⁺ T cells
CD45RA
FOXP3
I
II
III
C
CD4⁺ T cells
c30
CD45RA
FOXP3
D
Treg-Fr-I
Treg-Fr-II
Treg-Fr-III
P= 0.023
P= 0.913
P= 0.975
% of CD4⁺ T cells
AA
HC
E
CD4⁺ T cells
eTregs
Treg-Fr-I
Treg-Fr-II
tSNE2
tSNE1
F
Tregs
P= 0.003
R= 0.726
Fr- II (% of CD4⁺ T cells)
Fr- I (% of CD4⁺ T cells)
G
P= 0.064
R= 0.527
FEV1/FVC (% of predicted)
CD4_c30 (% of CD4⁺ T cells)
H
CM CD8⁺ T cells
EM CD8⁺ T cells
P= 0.004
R= 0.710
P= 0.011
R= 0.656
% of CD8⁺ T cells
Treg-Fr-I (% of CD4⁺ T cells)

FIGURE 5

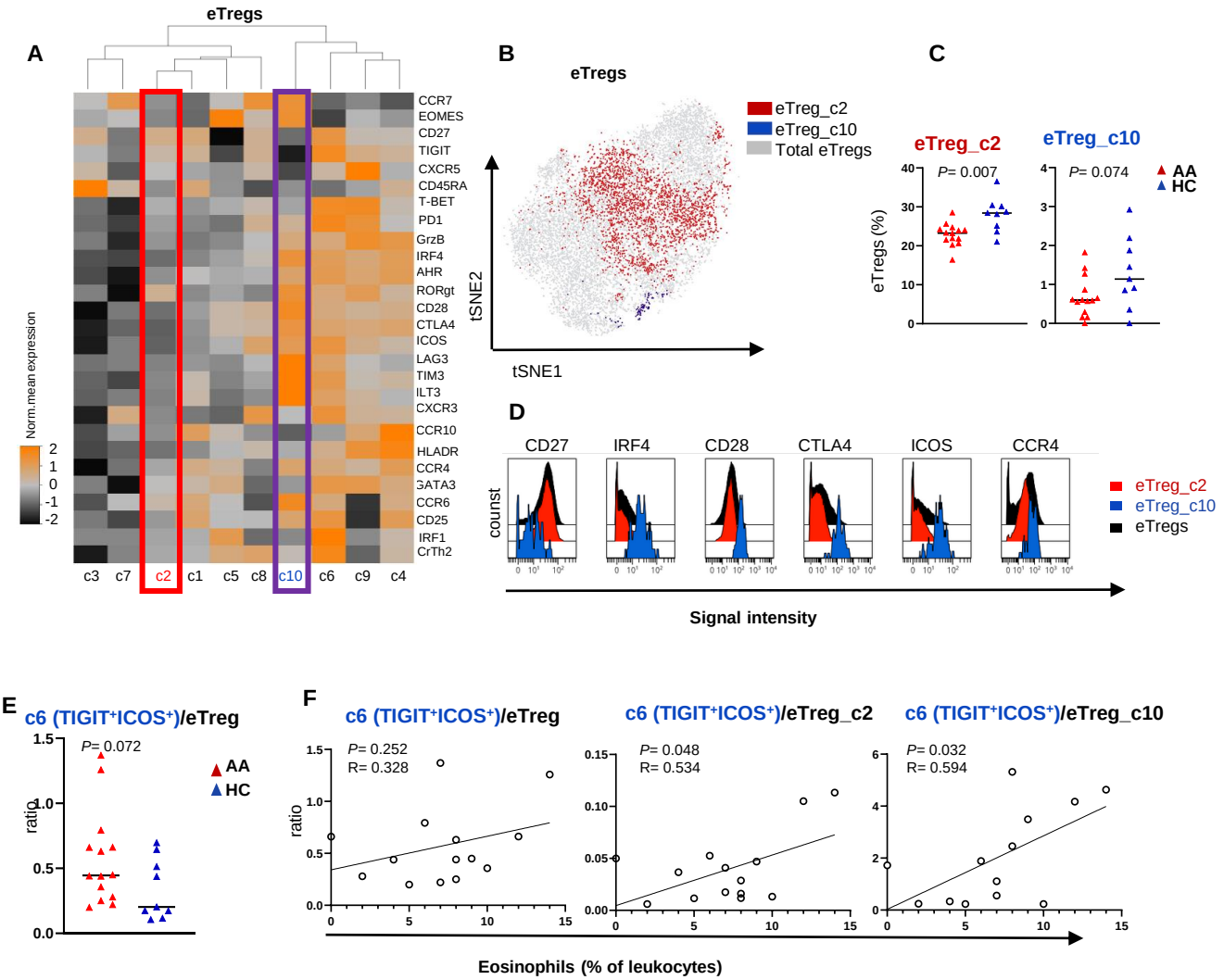
A
eTregs
CCR7
EOMES
CD27
TIGIT
CXCR5
CD45RA
T-BET
PD1
GrzB
IRF4
AHR
RORgt
CD28
CTLA4
ICOS
LAG3
TIM3
ILT3
CXCR3
CCR10
HLADR
CCR4
GATA3
CCR6
CD25
IRF1
CrTh2
Norm.mean expression
2
1
0
-1
-2
c3 c7 c2 c1 c5 c8 c10 c6 c9 c4
B
eTregs
eTreg_c2
eTreg_c10
Total eTregs
tSNE2
tSNE1
C
eTreg_c2
eTreg_c10
P= 0.007
P= 0.074
AA
HC
eTregs (%)
D
CD27
IRF4
CD28
CTLA4
ICOS
CCR4
counst
eTreg_c2
eTreg_c10
eTregs
Signal intensity

E
c6 (TIGIT+ICOS+)/eTreg
P= 0.072
AA
HC
ratio
F
c6 (TIGIT+ICOS+)/eTreg
P= 0.252
R= 0.328
c6 (TIGIT+ICOS+)/eTreg_c2
P= 0.048
R= 0.534
c6 (TIGIT+ICOS+)/eTreg_c10
P= 0.032
R= 0.594
ratio
Eosinophils (% of leukocytes)

FIGURE 6

A

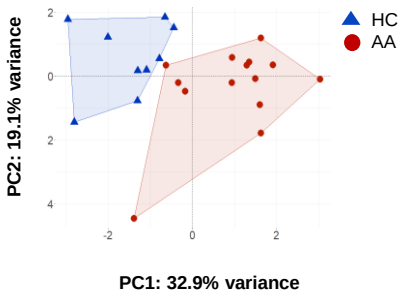

B

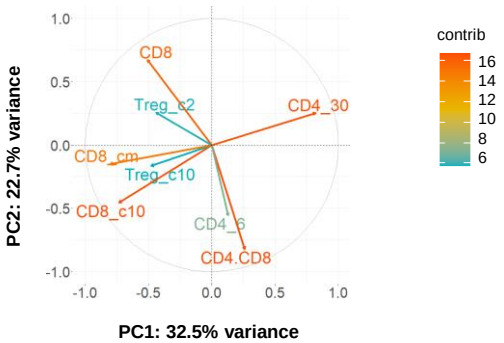

C

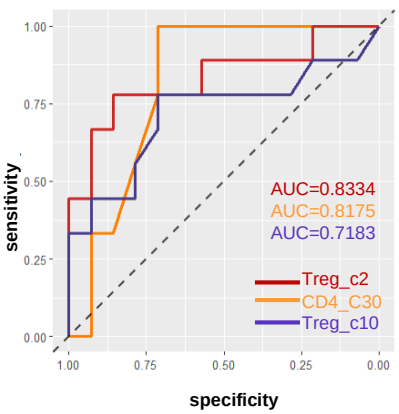

D